Vol. 685: 49–67, 2022
https://doi.org/10.3354/meps13970

MARINE ECOLOGY PROGRESS SERIES
Mar Ecol Prog Ser

Published March 10

Spatiotemporal scales of larval dispersal and connectivity among oil and gas structures in the North Sea

C. Gabriela Mayorga-Adame[1,*], Jeff A. Polton[1], Alan D. Fox[2], Lea-Anne Henry[3]

[1]National Oceanography Centre, Joseph Proudman Building, Liverpool L3 5DA, UK
[2]Scottish Association for Marine Science, Oban PA37 1QA, UK
[3]School of GeoSciences, Grant Institute, King's Buildings Campus, University of Edinburgh, Edinburgh EH9 3FE, UK

ABSTRACT: The ecological role of offshore man-made infrastructure is of growing international interest. By 2030, globally more than 7500 oil and gas platforms could be removed, many of which now host mature hard substrate ecosystems formed by sessile benthic species including sponges, corals and mussels. We investigated the spatiotemporal scales of generalised species dispersal and connectivity among oil and gas structures in the North Sea using strategically designed 3D advective passive particle tracking experiments forced by high resolution (1.8 km, hourly) velocity fields including tide-, density- and wind-driven currents. Trajectories from 2 seasonal releases during mixed winter (February) and stratified summer (July) conditions of 2010 were analysed for a variety of pelagic larval durations (PLDs) spanning 2 to 28 d. Particles dispersed on average 32 km away from their origins after just 5 d, 67 km after 15 d, and 109 km after 28 d, with considerable spatial variability and limited seasonal variations. Short (2 d) PLDs generated highly connected networks over smaller spatial scales, while longer PLDs (28 d) generated less fragmented networks covering a much larger area but with fewer connections. Tidally driven dispersal was isolated using a new method based on the harmonic analysis of the velocity fields: the resulting maximum linear dispersal distances varied from ~4 km in the northern North Sea to ~8 km in the southern North Sea. The present study provides baseline spatiotemporal scales of dispersal and connectivity patterns and optimized relocatable methods to assess connectivity in tidally active shelf seas.

KEY WORDS: Larvae · Dispersal · Connectivity · North Sea · Oil platform · Offshore infrastructure · Shelf sea · Harmonic analysis · Tidal motion

1. INTRODUCTION

1.1. Ecological services of oil and gas platforms and trade-offs of their removal

Studies on the ecological importance of offshore oil infrastructure are gaining international interest. By 2030, more than 7500 oil and gas platforms from at least 53 countries will become obsolete (Fowler et al. 2018), and the ecological impacts of their removal are not well known. Offshore platforms can enhance local biodiversity through provision of new hard substrate that over time can become colonised by macroalgae, mussels and colonial epifauna, forming reef-like habitats (Gates et al. 2017, Coolen et al. 2020a). The full depth of oil and gas platforms, including any subsea infrastructure, can be exploited by such flora and fauna from the surface to the seafloor, and vertical zonation and species turnover of these habitats is well documented (Torquato et al. 2017, Coolen et al. 2020a). The habitats these substrates now form may boost recruitment of overexploited commercial fish

*Corresponding author: gmaya@noc.ac.uk

Publisher: Inter-Research · www.int-res.com

species (e.g. rockfish *Sebastes paucispinis*; Love et al. 2006), they can produce fish biomass at enhanced rates (Claisse et al. 2014), act as foraging sites for top predators (Todd et al. 2009, Robinson et al. 2013) and provide protection from bottom trawling because they have fisheries exclusion zones around them. Besides these well-known localised reef effects, offshore oil and gas installations can act as vectors for non-native species of fish (e.g. Pajuelo et al. 2016) and invertebrates (e.g. Creed et al. 2017). Keeping obsolete structures in place on the seafloor creates hazards to seafarers and fishers, as well as a potential continued release of pollutants from the degrading structures. On the other hand, removing offshore platforms at the end of their operational lifetimes has several negative effects including decreasing hard substrate availability for reef-associated communities, atmospheric emissions and economic costs of the removal process, re-suspension of contaminated sediments, possible contribution to the spread of invasive species and reduction of biological connectivity (Macreadie et al. 2011, Fowler et al. 2014). Failure to adequately account for both positive and negative impacts of the removal of obsolete structures, or the addition of new structures, could have serious consequences for offshore ecosystems, including biodiversity loss and further depletion of fish stocks (Fowler et al. 2018).

The trade-off between positive and negative impacts of offshore oil and gas structures removal has to be established for each specific region taking into account economic, ecological and societal impacts (Fowler et al. 2018), particularly in the Northeast Atlantic which is covered by the OSPAR Convention. OSPAR Decision 98/3 on the Disposal of Disused Offshore Installations requires full removal of offshore oil and gas infrastructure, except for pipelines, unless conditions for derogation can be met. A recent panel of international experts on just the environmental aspects advised that a flexible approach to decommissioning should be based on an assessment of relative net environmental benefit, taking into account the ecological services provided by offshore structures, their potential detrimental effects, as well as the impacts of removal (Fowler et al. 2018). They agreed that if a group of installations is ecologically interconnected, then decommissioning options for these structures should be considered in relation to each other rather than on a structure by structure basis. Ecological connectivity is recognized as an important factor in determining decommissioning strategies (McLean et al. 2022); however, to our knowledge, no studies have addressed this issue at the regional scale of the North Sea from a generic point of view. However, a few studies on regional connectivity of these structures have been put forward for species of conservation interest (e.g. *Lophelia pertusa*; Henry et al. 2018), or considering the full spectrum of anthropogenic structures including the numerous shipwrecks in the North Sea, which now provide similar reef-like habitats (e.g. van der Molen et al. 2018). Considering the uncertainty that remains in larval biology, a more generalised approach looking at the possible range of dispersal and connectivity, specifically among oil and gas structures in the North Sea for a range of pelagic larval durations (PLDs), is needed. This study aims to provide baseline information applicable to passive substances or organisms originating at oil and gas structures with a variety of dispersal periods that could serve as a starting point for more complex multispecies larval connectivity studies.

1.2. Marine connectivity drivers

The dynamic ocean is responsible for the dispersal of passive particles drifting on it. Dispersal can be considered as the effect of all processes responsible for transporting (advecting) and spreading (diffusing) a cloud of particles. These processes include large-scale advection by density-, tide- and wind-driven currents, and small-scale (randomized) motions (or mixing) by waves and turbulent processes. These processes are highly variable in time and space, leading to similarly complex patterns of dispersal. The dispersal of marine larvae is not only controlled by physical flow parameters but is also influenced by temperature, and biological processes such as the timing of spawning, PLD, and larval behaviour, (Phelps et al. 2015b, James et al. 2019), mortality (Mayorga-Adame et al. 2017, Gary et al. 2020), and settlement ability (Abelson & Denny 1997, Leis & Carson-Ewart 1999). The net combined effect of these processes determines the spatial scales over which a population is connected (Gawarkiewicz et al. 2007). This study focusses on the larger-scale motions produced by advection due to the 3-dimensional velocities of a high-resolution ocean model (Guihou et al. 2018) while the effects of diffusion due to subgrid-scale motions are not addressed.

1.3. North Sea characterization and dynamics

The North Sea is a semi-enclosed shelf sea that lies between Norway, the European Continent and the

British Isles. It is a shallow sea, with depths of 80 m or less in the southern North Sea, whereas the northern North Sea reaches depths of 160 m. Only the Norwegian trench on the eastern side has a depth >250 m, with a maximum of 600 m in the Skagerrak (the area between Denmark, Sweden and Norway). The general circulation pattern in the North Sea and the Skagerrak is mainly cyclonic, and while the circulation pattern in winter and summer differs in detail, the seasonal patterns are similar (e.g. no major reversals) (Fig. 1). Atlantic and Celtic Sea warm salty water comes into the North Sea through the northern boundary and the English Channel, where it mixes with fresh waters from rivers and brackish water from the Baltic outflow (Winther & Johannessen 2006). The northern boundary main inflow comes as a subsurface flow along the west slope of the Norwegian Trench, recirculates, without mixing with the rest of the North Sea, and leaves along the eastern slope. The surface inflow comes in east of the Shetland Islands, and through the Fair Isle Passage, between the Shetland and Orkney Islands. About 76% of this inflow goes eastward to form the northern recirculation cell along the 100 m isobath known as the Dooley Current. The remaining 24% continues southward to form the central recirculation cell along the ~50 m isobath, north of the Dogger Bank (Mathis et al. 2015). Only ~5% of the northern inflow reaches the Southern Bight in the southern North Sea, where it converges with the English Channel inflow and continues flowing through the German Bight up to northern Denmark (Mathis et al. 2015). There it joins the flow of the central recirculation cell forming the Jutland Current, which enters the Baltic Sea through the Skagerrak, forming a cyclonic eddy (Mathis et al. 2015). Reviewing the magnitude of inflows and outflows, Huthnance (1997) concluded that flushing time of the North Sea is ~9 mo, with significant spatial variability.

Tidal motion is the dominant dynamical feature of the North Sea. Tides have an oscillatory nature, which can directly connect regions on small spatiotemporal scales (hours, 100s of m to a few km). Tidally induced mean currents, usually referred to as residual currents, can produce longer-distance connections (see e.g. Polton 2015 for a discussion on the associated mechanisms in this region). In the North Sea, much of the area experiences residual currents with magnitudes between 1 and 5 cm s^{-1}. Tides can also enhance vertical mixing, from the seabed upwards, in shallow shelf seas. This mixing can significantly influence the dispersal and lateral transport of plankton that could otherwise only relocate with vertical

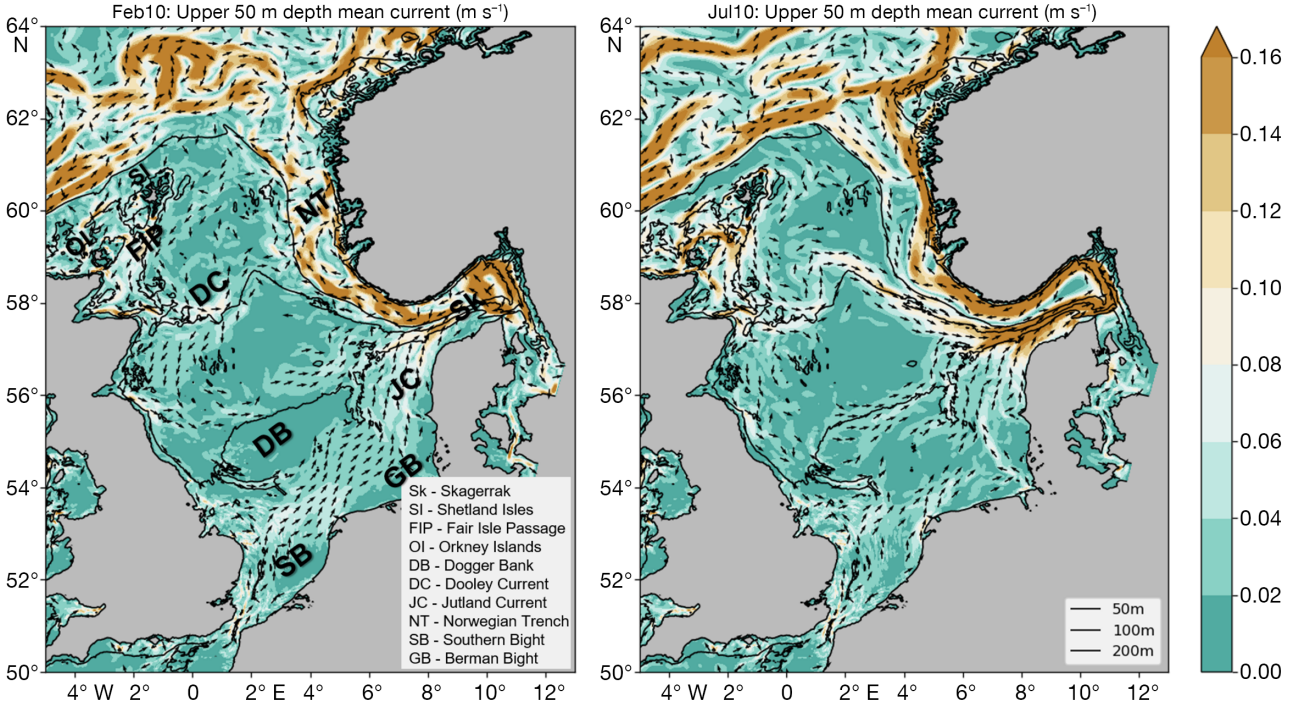

Fig. 1. The North Sea and its seasonal variation in near-surface currents. The colour scale represents the speed in m s^{-1} of the time and depth average currents in the upper 50 m for February and July 2010, representative of the northern hemisphere winter and summer conditions, respectively. Vectors are shown to illustrate the flow direction for speeds higher than 0.02 m s^{-1}. Data are from the NEMO AMM60 (1/60°) model configuration (Guihou et al. 2018)

migration. Diel vertical migrations common to several species of zooplankton and some planktonic larvae may interact with the tide in such a way that considerable net transports of larvae result, even in the presence of just alternating tidal currents subject to bottom shear (Bowden 1965, Young et al. 1982, Otto et al. 1990). The dominant tidal component in the North Sea is the semi-diurnal M2, although it is relatively small in the Norwegian sector. In the southern North Sea, the M2 tidal flows are almost rectilinear (elliptical eccentricity ~0.98), reaching speeds of 1 m s^{-1}, and generating enough bottom boundary layer turbulence to mix the entire water column. In the UK sector of the northern North Sea, eccentricity is lower (~0.75) and tidal flows are smaller (~0.25 m s^{-1}) which allows for seasonal stratification (Thorpe 2012).

A strong seasonal signal dominates the sea surface temperature variability in the North Sea, with means (±SD) of 7.02 ± 0.48°C and 13.62 ± 0.60°C in winter and summer, respectively (Mathis et al. 2015). It is most obvious in the southern and eastern coastal regions and is mainly determined by heat exchange with the atmosphere. In the shallow southern North Sea (away from coastline freshwater sources), temperature is vertically mixed all year round, while in the northern North Sea, a summer thermocline develops at around 30–40 m depth (Quante et al. 2016).

Historically, it was thought that the long-term circulation in the North Sea was generally weak and driven by episodic storms (Simpson 1981). Subsequently, the role of the thermohaline circulation on shelf seas was identified (Brown et al. 1999, Hill et al. 2008), and now density-driven frontal jets are recognized as having the most significant contribution to seasonal shelf transport in the North Sea (Hill et al. 2008). In summer, spatial variations on tidal mixing generate patches of stratified and vertically homogeneous waters, separated by sharp tidal mixing fronts with both a surface temperature, a more persistent bottom salinity expression and strong frontal jets parallel to them. The bottom density gradient drives, by thermal wind balance, a near-surface cyclonic geostrophic jet above the bottom fronts (Hill et al. 2008). In the North Sea, jets produced by this mechanism have been observed with drifters, reaching speeds of up to 0.3 m s^{-1} at depths of typically 30 m below the sea surface (Brown et al. 1999, Hill et al. 2008). The sensitivity to climate forcing of thermohaline processes driving shelf sea circulation has been investigated by Holt & Proctor (2008) and Holt et al. (2018).

The interannual variability in the general circulation of the North Sea is driven mainly by varying local wind conditions, including storms, interacting with the Atlantic water masses inflow. It is therefore heavily influenced by the large-scale atmospheric North Atlantic Oscillation (NAO). In the North Sea, positive NAO phases are associated with higher air temperatures and stronger westerly winds, which induce higher water temperatures, high sea levels, and generally enhanced circulation flows, and shelf edge currents (Mathis et al. 2015). Notably, the NAO phase is also associated with significant variation in the potential for larvae in the North Sea to disperse and form connections to downstream populations (Fox et al. 2016).

1.4. Study approach and objectives

This study is a numerical experiment in response to the theoretical preliminary assessment of the biological connectivity among oil and gas platforms in the North Sea put forward by Thorpe (2012), which provides theoretical estimates of the scales of biological connectivity. The purpose of this study is to investigate the spatiotemporal scales of connectivity among oil and gas structures in the North Sea, taking advantage of the new generation of high-resolution ocean circulation models at the kilometric scale. In doing so, we also investigated biological connectivity potential, driven solely by tidal motions.

There are more than 1000 offshore oil and gas structures in the Greater North Sea region to date (OSPAR database; see 'Data availability'), excluding pipelines but including platforms, manifolds and wellheads, mostly made of steel or concrete. We used a Lagrangian particle tracking modelling approach to empirically investigate the connectivity among these structures. Trajectories were analysed to determine the interconnectedness among the subsea structures for different temporal scales and seasons of the year 2010 (see Fig. 1 for the contrasting circulations). There were no significant weather events during these seasons. Indeed, winter 2009/10 was marked by prolonged blocked anticyclonic weather patterns (Kendon & McCarthy 2015) creating cold, calm and snowy conditions.

Results of this Lagrangian particle tracking study are expected to provide improvements in comparison to previous studies, since we used output currents from the new generation of high-resolution ocean circulation models (at the kilometric scale) which provide a more realistic representation of the ocean flows (Guihou et al. 2018). Results are presented in a generic way, intended to be useful as a starting point for analysing the connectivity among the subsea oil and gas structures for passive substances or organ-

isms spending different amounts of time in the water. The spatiotemporal scales and patterns of connectivity due to 3-dimensional advection by the complex modelled flow are presented. Since tidal flows are expected to be one of the main drivers of connectivity in shelf seas, connectivity due to tidal currents is isolated using a multicomponent harmonic analysis method that does not require particle releases. Results are discussed in light of expected inter-annual variability due to large-scale atmospheric fluctuations, particularly the NAO, and expected changes in local circulation patterns and stratification due to climate change.

2. METHODS

2.1. Lagrangian particle tracking experiments

Particle tracking experiments to simulate the dispersal of passive particles originating from oil and gas platforms in the North Sea were conducted using a version of the Lagrangian TRANSport model (LTRANSv.2b; North et al. 2011). The LTRANS code was modified to work with 3-dimensional velocity output from a high-resolution NEMO ocean circulation model (https://www.nemo-ocean.eu) configuration for the North West European Shelf, the Atlantic Margin Model 1/60° (AMM60; Guihou et al. 2018). This ocean circulation model has a horizontal resolution of approximately 1.8 km and 51 hybrid-σ-vertical levels with a realistic bathymetry from GEBCO. The model includes ERA-interim atmospheric forcing (6-hourly wind velocities and 3-hourly air temperature, humidity, radiative fluxes, and precipitation fields with a spatial resolution of ~97 km), TPXO7.2 tidal forcing, open boundary forcing from the northern North Atlantic basin configuration, and daily freshwater influx from 322 rivers (synthesized from the Global River Discharge Data Base; Vörösmarty et al. 2000) and gauge discharge data prepared by the Centre for Ecology and Hydrology) (see Guihou et al. 2018 for further details). Hourly velocity fields were archived for the particle tracking experiments to ensure the accurate representation of the strong tidal flows, characteristic of the region.

An open-access list of offshore oil and gas structures (OSPAR database) was used to generate an initial list of release locations; after removing repeated locations, a list of 954 platforms (nodes) was kept (Fig. 2). Particles were released at these locations, 0.5 m beneath the sea surface at midnight during 14 consecutive days in the months of February and July, in order to cover a complete spring–neap tidal cycle (~14 d), during a month representative of the winter (mixed) and summer (stratified) conditions. Releasing at a fixed time each day results in a phase shift in the release time relative to the tidal phase (the apparent shift is approximately 1 h d^{-1}), thereby releasing particles over all phases of the semi-diurnal tide. Near-surface particles are used to maximize dispersal potential and to mimic buoyant, ubiquitous eggs and larvae. The number of particles released added up to 142 520 particles mo^{-1} (140 per subsea structure). Particles were advected by the hourly 3-dimensional velocity fields and tracked for 30 d with a time-step of integration of 10 min, and their along-track position was stored every half an hour.

2.2. Post-processing analysis

Particle tracks were grouped by release month and aligned in the time dimension according to the time they spend in the water (not by their release date). To make a generic and comprehensive analysis applicable to a variety of processes of different duration (i.e. PLDs), linear distance from source was calculated every day for the 28 d trajectories (see Fig. 3). To show the spatial variability, mean linear dispersal distances for each platform were calculated from the trajectories of the 140 particles released per structure for trajectory lengths of 5, 15 and 28 d (see Fig. 4). To abbreviate, PLD is used interchangeably with particle tracking duration within the text.

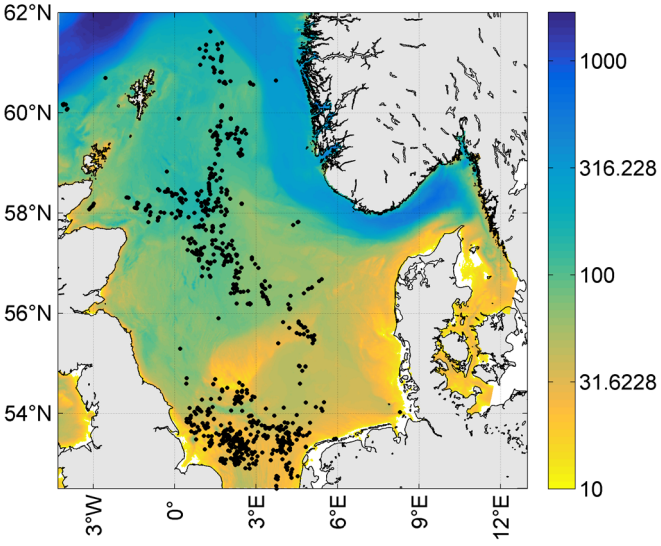

Fig. 2. Locations of oil and gas platforms in the North Sea (OSPAR database) used as seeding locations for particle releases. The colour shows North Sea bathymetry (m) as represented in the AMM60 model (note the log scale)

To construct connectivity matrices, particles were evaluated for settlement every 2 d along the 28 d particle trajectories, considering a 2 d competency period (the period of time when larvae are suitable for settlement). Settlement evaluation was performed every 30 min during the competency period. Particles were considered to successfully settle on a subsea structure if they were found within a 1 km radius of a structure location at any given time during the competency period. This radius is less than the tidal connectivity footprint (see Section 3.3). Furthermore, considering sensitivity analysis carried out by Mayorga Adame et al. (2017) and the potentially large size of the oil and gas structure, a 1 km radius is a conservative assumption.

A single particle is assumed to represent a packet of larvae; therefore, settled particles were not removed from the system to allow onward connections from the same 'larval packet'. Since particles could potentially settle every time they were evaluated (96 times, every 30 min during 2 d of competency) in the same or different structures, the number of particles arriving at each platform was normalized dividing by the number of settlement opportunities, to get a probability of settlement in any given platform. This probability was recorded into connectivity matrices to characterize the strength of the connections among platforms. Connection strength was then normalized by the maximum number on that connectivity matrix to produce scaled values between 0 and 1. The binary version of the connectivity strength matrices, containing only zeros and ones to mark existing connections, was used to calculate the number of unique structure-to-structure connections (see Fig. 9). Unique connections represent 'all plausible connections' equally weighted. This is an important metric since the number of particles simulated will always be limited, and a connection observed once in the model is highly likely in the real ocean. Furthermore, from an evolutionary perspective, a true unique connection in the real ocean, with later reproductive success will have a disproportionate effect on a population. Self-seeding, i.e. the number of particles retained at the origin location, was also calculated (see Fig. 10).

2.3. Network metrics

The resulting connectivity matrices were visualized as networks, and several network metrics, including degree, betweenness, centrality and modularity, were calculated and explored using the free network visualization software Gephi (Bastian et al. 2009; https://gephi.org). The distribution of network metrics and its variability with tracking length (PLD) was visually explored. Highly connected clusters among the networks were identified using the Louvain modularity metric (Blondel et al. 2008), which uses a resolution parameter (Lambiotte et al. 2009) to determine the number of clusters selected. Since our networks appeared relatively insensitive to the choice of resolution parameter, the default value of 1.0 was used. To characterize the fragmented networks, simple degree and weighted degree metrics were used. Degree is the sum of connections emanating from a node (out-degree) and coming into a node (in-degree). Weighted degree is similar, but the strength of the connections is included as a weight. The ratio of in-degree to out-degree (RIOD) was also calculated. While these are simple metrics compared to higher-level centrality measures (e.g. betweenness, eigenvector centrality and PageRank), they have the advantage of retaining straightforward ecologically relevant information: high degree identifies nodes connected to many other sites, weighted degree gives an idea of the relative numbers of recruits or the proportion of released larvae that subsequently settles successfully, and RIOD helps identify platforms acting mainly as sources (RIOD < 1) and differentiate them from those acting mainly as sinks (RIOD > 1), or equally as sinks and sources (RIOD = 1).

2.4. Tidal connectivity

Since the highest number of unique connections is generated by the shortest trajectories (see Fig. 9), we investigated the connectivity arising solely from tidal motions. To do this, surface tidal velocities were reconstructed using the results of the AMM60 harmonic analysis at the location of the oil and gas structures. For each location, a time-series of velocity was evaluated over 270 d to capture the most significant variability from the oscillatory harmonic tides. For each location, under an assumption of spatially homogeneous velocities over the lateral tidal excursion range, we obtained a path representing the tidal procession of a particle. The area swept by this path is characteristic of a particle released at that specific phase of the dominant semi-diurnal tide. (i.e. the 'centre of mass' of the path is largely described by the direction of flow at the time of particle release). The path evaluation was repeated for starting times varying over all phases of the semi-diurnal tide (mimicking particle tracking releases at different tidal phases). A footprint of tidal advection, for each

structure, is then defined as the polygon bounding all along-path positions. This tidal footprint is an estimation of the area around a point that is swept by tidal currents and that is therefore dynamically connected at the short time scales of a tidal cycle. When 2 or more structures lie within a tidal footprint, they are considered to be directly connected by tides, since during a tidal cycle material originating from either of these structures could come into contact with the other structure. If the tidal footprints of 2 or more structures overlap, they are considered to be indirectly connected by tides. Material originating from these platforms has the potential to mix; however, their simultaneous convergence in the overlapping region of the tidal footprint would normally be prevented for a simple 2-dimensional advective flow, since the region would be occupied at different phases of the tide by material from each footprint. However, horizontal mixing and vertical displacements (due to e.g. sinking, diel vertical migration, tidal vertical migration, mixing) would likely cause this interaction to occur. Here, both direct and indirect tidal connections are equally considered, and the tidal footprints of tidally connected structures are joined to estimate tidally connected areas. This tidally connected scale gives an estimate of how far material emanating from a structure can spread in a tidal cycle.

3. RESULTS

3.1. Spatiotemporal scales of dispersal and seasonal changes

Mean linear dispersal distance measures how far away from the origin location particles can reach after a given period of dispersal. It gives a general spatial scale of how far passive eggs, larvae or neutrally buoyant pollutants would reach after some time in the water. On average, considering all platform locations and both the winter (February) and summer (July) releases, particles disperse 32 km radially away from their platforms of origin after 5 d in the water, 67 km after 15 d and 109 km away after 28 d of dispersal (Fig. 3). Mean linear dispersal distance is larger for the winter releases in the first 20 d of dispersal, while for larger PLDs, summer releases show larger mean linear dispersal distances. The maximum difference in mean linear dispersal distance between the seasonal releases is 14 km after 12 and 28 d of dispersal, although these differences are relatively small compared to the standard deviations, which are similar for releases in both seasons. The standard deviation increases with time in the water to 66 and 68 km after 28 d in the water in the February and July releases, respectively.

Minimum linear dispersal distance after 28 d in the water is <1 km for both seasons, which indicates a potential for retention around the platforms, even with 3-dimensional flows that include a non-oscillatory wind-driven component. The maximum linear dispersal distance travelled by a particle exceeds 130 km after 5 d of dispersal, 300 km after 15 d for both seasonal releases and up to 560 km after 28 d in the February release and 780 km in July (corresponding to about 5 and 7 degrees of longitude in this region). These are extreme values but illustrate the maximum potential reach of material originating at the structures.

The spatial distribution of mean linear dispersal distance from the platform of origin for different length trajectories shows the spatial variably of the dispersal potential at different platform locations, and their seasonal variation, depending on the release month (Fig. 4). It illustrates how far passive materials released at the structures could reach, depending on their location of origin, and the dispersal period or age in the water, which for eggs and larvae equates to PLD.

Hotspots of long dispersal distance are located in the southern North Sea near continental Europe, and in the northern North Sea southeast of Orkney Island. Structures in these areas consistently show the longest dispersal distance for all dispersal periods and seasonal releases. The few structures located close to the Norwegian Trench current also

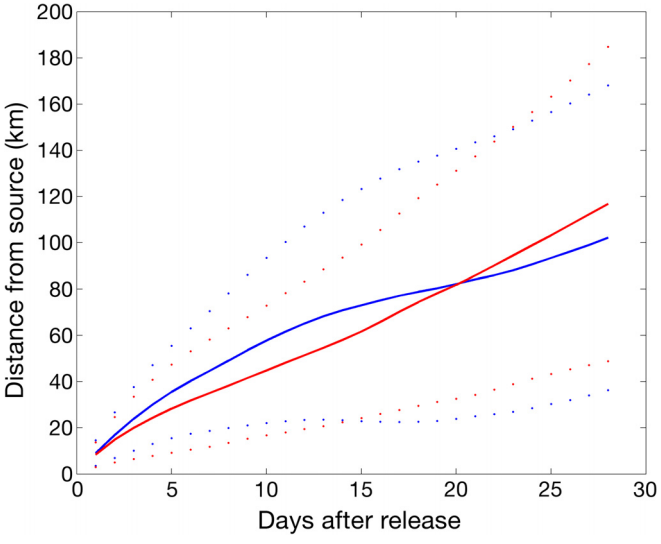

Fig. 3. Mean (solid lines) ± SD (dotted lines) linear dispersal distances of all particles released from oil and gas platforms in the North Sea as a function of time in the water for the winter (February; in blue) and summer (July; in red) releases

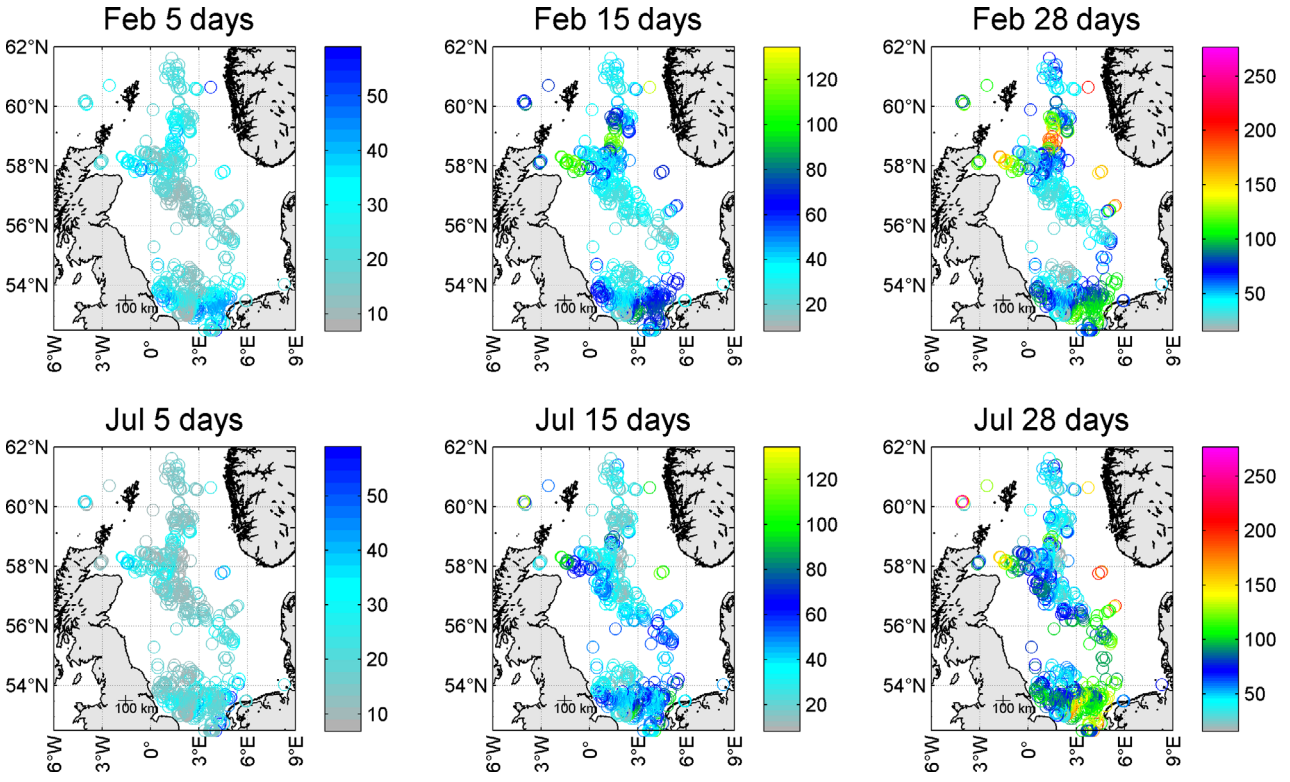

Fig. 4. Mean linear dispersal distances in kilometres (according to the staggered colour scale) from the platform of origin after 5, 15 and 28 d dispersal for the February and July releases

show strong dispersal due to the fast flows there. Other areas of long-distance dispersal, more prominent in the February release, are located in the northern North Sea around 59° N, and near the southeastern coast of England. In general, the central North Sea (between 58.5 and 54° N) is less dispersive, with particles staying around 50 km from their origins after 28 d of dispersal. Only in the July release did particles from structures in the eastern central North Sea disperse more than 100 km after 28 d in the water. The range of dispersal distance among platforms increases as the dispersal period increases, spanning 7–59 km after 5 d, 8–134 km after 15 d and 16–278 km after 28 d of dispersal. This was expected, since particles are carried away by currents, travelling longer distance over time; however, there is always some retention potential due to tidal recirculation.

Seasonal variability is more noticeable in the trajectories of particles released at subsea structures in the central and northern North Sea (Fig. 5). After 5 d of dispersal, some particles released in February show longer trajectories than those released in July 2010. Over time, in the northern North Sea, a stronger south-westward displacement is observed in the winter (February) release when some particles approach the southern Norwegian coast. Particles released at structures in the central North Sea (between 56 and 59° N) show the opposite pattern, dispersing further away in the summer release but towards the northeast (Fig. 5). In the shallow southern North Sea, the trajectories in the winter and summer releases are more similar, with a general westward displacement. Trajectories in this area show a more pronounced tidal influence in comparison to central and northern North Sea regions, characterized by more oscillatory trajectories due to the comparable strength of the directional density and wind-driven currents and the oscillatory tidal currents (Fig. 6).

The main current patterns in the North Sea remain constant throughout the year with increased strength in the winter months (Fig. 1). The main seasonal variation is vertical stratification, which occurs during summer in the central and northern North Sea at depths greater than 40 m (Fig. 7). The spatiotemporal variation in stratification explains the observed seasonal differences in trajectories in the central and northern North Sea, as well as the minimal seasonal variability in the shallow southern North Sea, which remains vertically mixed throughout the year.

Internal tides are resolved at the model resolution (Guihou et al. 2018), and the associated vertical

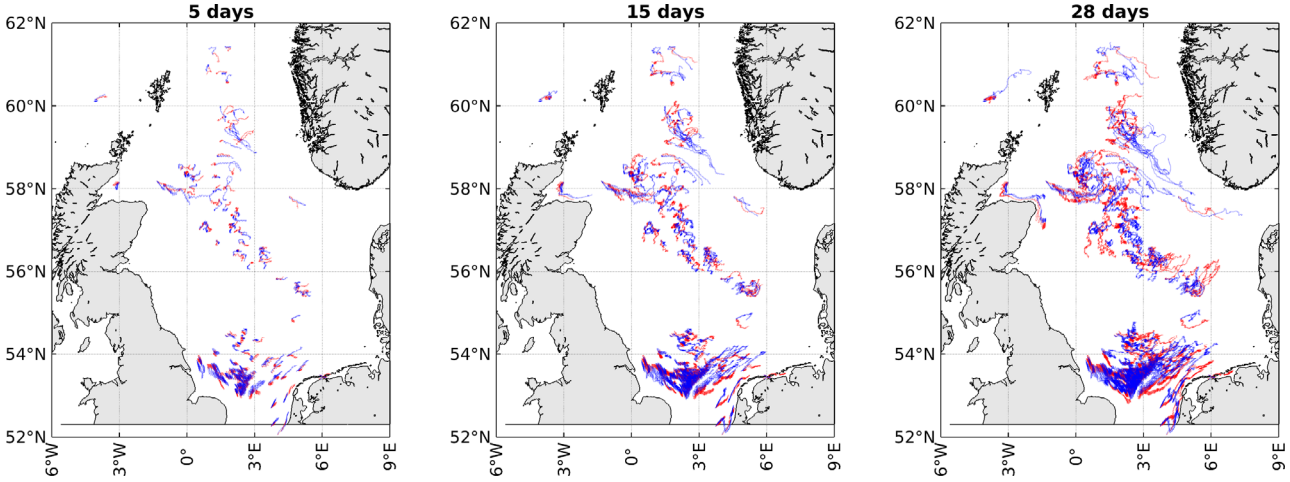

Fig. 5. Trajectories of 5, 15 and 30 d of some of the particles released in February (blue) and July (red)

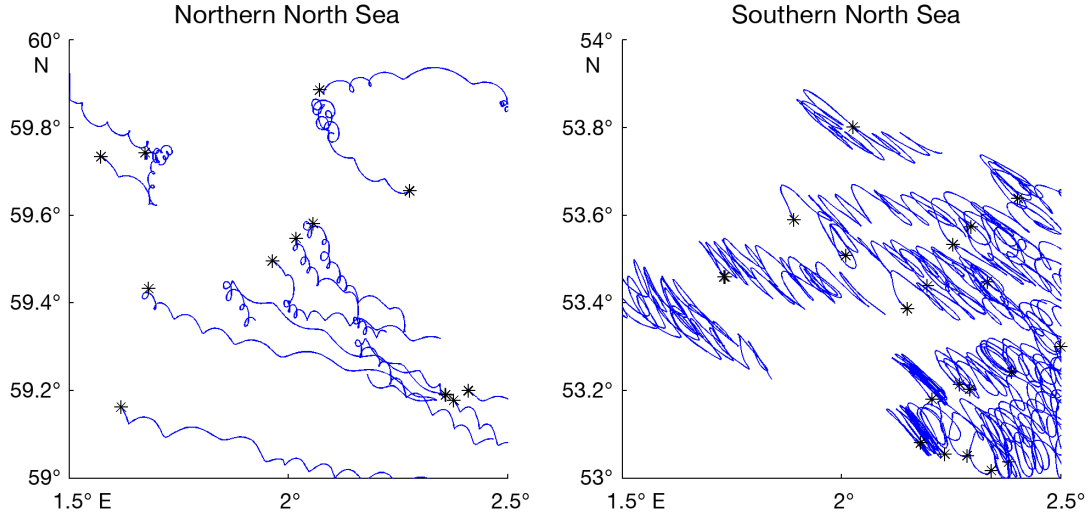

Fig. 6. Example of zoomed-in trajectories of particles in the northern and southern North Sea released in February

velocities (with a monthly mean amplitude in excess of 10 m d^{-1} along the edges of the Norwegian Trench, and elevated in the winter) provide a plausible mechanism for generating a spatially variable pattern of vertical dispersal of passive particles (Fig. 8). Following their near-surface release, in the southern North Sea, the average particle remains in the upper 12 m in both seasonal releases (Fig. 8; mean ± SD depth of 8 ± 8 m after 28 d of dispersal in February and 11 ± 10 m in July), while in the central and northern North Sea there is a strong seasonal variation in the depth trajectories, with the average particle remaining in the upper 3 m during the stratified summer (3 ± 3 m depth after 28 d of dispersal in the July release), but dispersing vertically in the water column down to 17 ± 32 m depth in winter (February release) (Fig. 8). The maximum depth reached by the particles released in the southern North Sea is 71 m in the winter release and 68 m in summer, while in the central and northern North Sea, the maximum depth fluctuates between 390 m in winter and 64 m in summer. The resulting vertical distributions expose particles to different horizontal velocity regimes, particularly in stratified shear flows; hence lateral dispersal is also affected by the depth varying advective flow, resulting in both vertical and horizontal spreading (apparent diffusion).

3.2. Connectivity networks

Evaluating connectivity for a range of PLDs between 2 and 28 d (considering 2 d of competency in which connections are evaluated every 0.5 h)

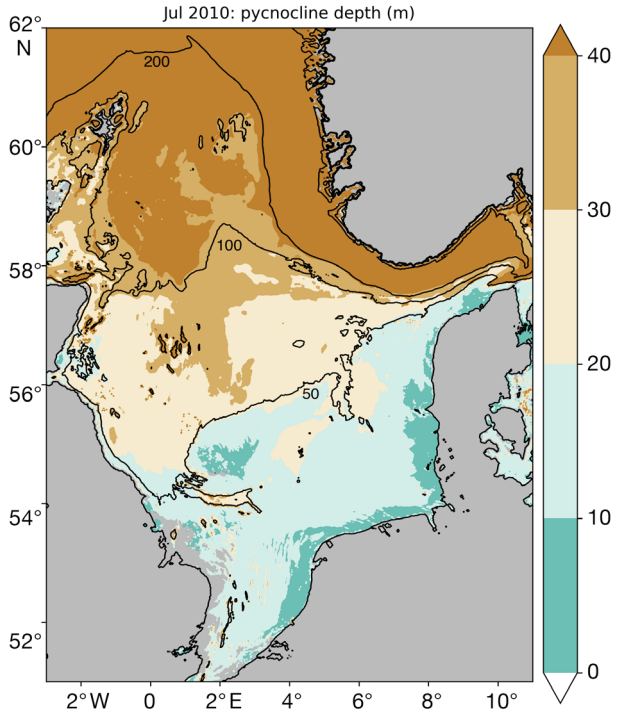

Fig. 7. Average pycnocline depth (m) for the month of July 2010. White regions represent full water column mixed regions, where the maximum density gradient was <0.01 kg m^{-4} throughout the month. Isobaths at 50, 100 and 200 m are shown for reference

shows that the number of unique pairwise connections between structures tends to decrease with longer PLDs (Fig. 9). Given the distributions of oil and gas structures and the hydrodynamics of the system, short PLDs of about 2 d produce the highest number of unique connections in both seasons. In the February release, however, a peak is also observed for PLDs of 12 d. The system seems to be slightly more interconnected in winter, particularly for PLDs of 10–16 d (Fig. 9). The maximum number of unique pairwise connections (6327 for 2 d PLD in July) represents 0.7% of all possible structure-to-structure connections, while the minimum (2980 for 26 d PLD in February) corresponds to 0.3%. Some of the connections realized at short PLDs are due to tidal dispersal (see Section 3.3). Self-seeding is partially responsible for the decrease of connections with trajectory length, as well as some of the seasonal differences (Fig. 10). As expected, the number of platforms retaining particles within the 1 km settlement ratio decreased rapidly with trajectory length; for 2 d PLD, 83% of the structures showed self-seeding in February and 88% in July, and this percentage decreased to 5 and 8%, respectively, for 4 d PLD, and continued to decrease to <0.3% for 28 d PLD (Fig. 10).

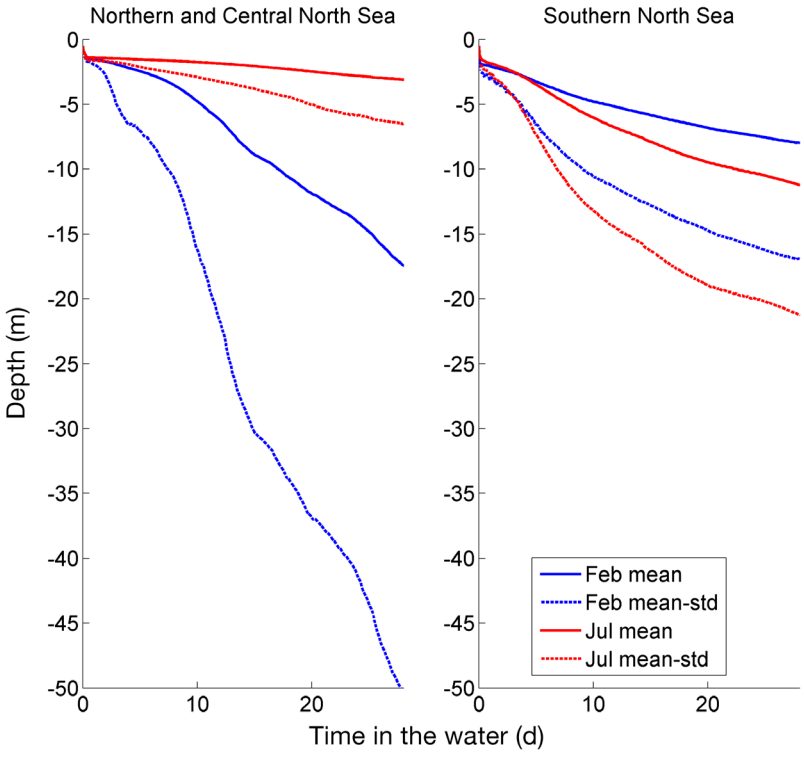

Fig. 8. Mean and SD (lower bound) of the vertical distribution of particles released from northern (latitude >56.25° N) and southern (latitude <56.25° N) North Sea subsea platforms. All particles are released 0.5 m below the surface

The resulting connectivity matrices are visualized in Fig. 11 as geolocated networks using Louvain modularity to identify highly connected clusters (colour), and the RIOD to identify installations acting mainly as sources (larger circles), installations acting mainly as sinks (medium size circles) or equally as sinks and sources (small circles). This visualization shows that connections to distant platforms (marked with lines in Fig. 11b,d) increase with tracking time (~PLD). The networks formed by the 2 and 28 d trajectories illustrate the observed variability for both winter and summer releases (Fig. 10). Despite having the highest number of unique connections (Fig. 9), higher average degree (6 in February and 11 in July), and weighted degree (3 in February and 4 in July), the network formed by 2 d trajectories is much more fractionated than the one formed with longer trajectories; the modularity metric of the 2 d network reveals 28 communities including more than 1% of the platforms in

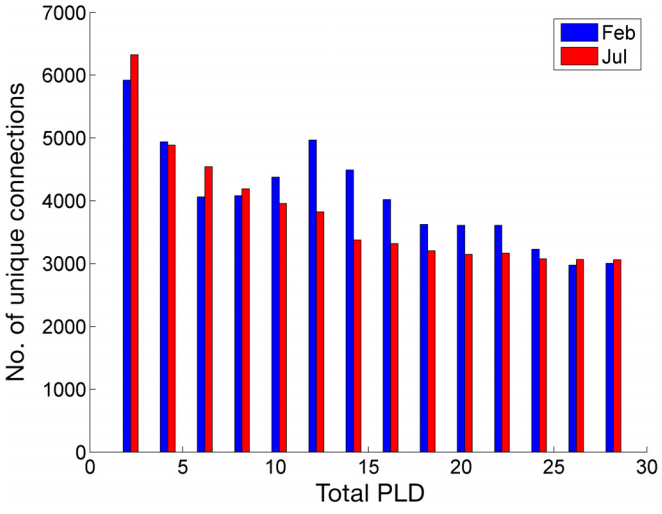

Fig. 9. Number of unique pairwise connections extracted from the binary connectivity matrices for different total pelagic larval duration (PLD), composed of a varying pre-competency period (every 2 d between 0 and 26 d) plus a competency period of 2 d, in which particles are evaluated for settlement into 1 km radius circular polygons around the platforms, every 30 min

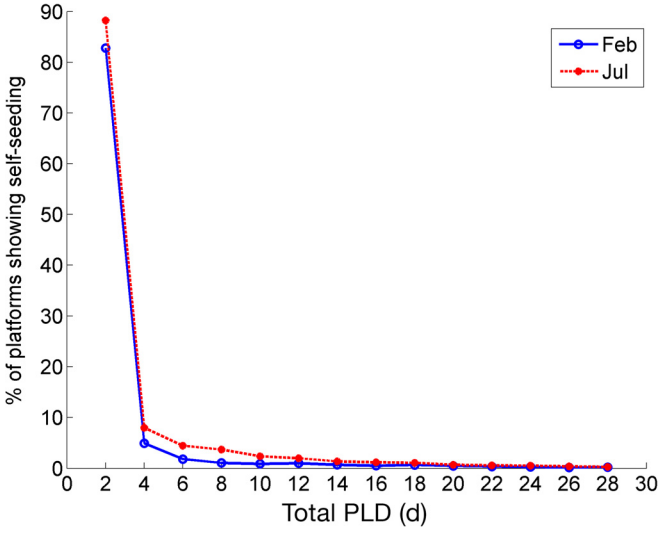

Fig. 10. Percentage of platforms showing self-seeding for total pelagic larval durations (PLDs) between 2 and 28 d

the February experiment (coloured clusters in Fig. 11a), and 29 in the July experiment (Fig. 11c). Clusters are spatially restricted, and the largest one includes only 6% of the structures in the February experiment and 7% in July. There is no clear regional distribution of structures acting mainly as sources and structures acting mainly as sinks, or equally as sinks and sources (circle size distribution in Fig. 11).

The number of long-range connections increases with tracking length; therefore, the overall connectivity of the network increases for longer trajectory lengths (Fig. 11c,d), despite the decrease in the number of connections and their strength as indicated by the average degree (3 in both seasonal experiments) and average weighted degree (0.23 in both seasonal experiments) and the decrease in the number of unique connections (Fig. 9). The network formed using particle trajectories of 28 d (including 2 d of competency) shows larger highly connected clusters in the north, central and southern North Sea, in both February and July experiments. The winter network is more strongly connected, with 12 clusters including >1% of the structures identified by the modularity metric and the largest one containing 14% (Fig. 11b), in comparison to the summer network, with 15 strongly connected communities and the largest cluster containing 16% of all structures (Fig. 11d). The largest cluster in both summer and winter experiments is centred at 58° N, but in February it includes more structures located to the east, while in July it includes a few more structures to the south. The networks formed by 28 d trajectories show a weak longitudinal pattern of the RIOD metric, with structures acting as sources (larger circles in Fig. 11) predominantly located at the western side of the North Sea basin and structures acting mainly as sinks (medium size circles in Fig. 11), or equally as sinks and sources (smaller circles in Fig. 11), at the eastern side. This pattern is especially noticeable in the southern North Sea. The network configuration of the northern North Sea shows the strongest seasonal variations, as expected from the seasonal changes in stratification and circulation.

3.3. Tidal connectivity based on harmonic analysis

The tidal footprints are much larger in the shallow southern North Sea, with an average major axis of 5.1 ± 2.1 km (mean ± SD) and areas of 7.2 ± 7.3 km^2 in comparison to 3.0 ± 1.2 km major axis and 3.7 ± 2.9 km^2 areas in the northern North Sea. Tidally connected areas reach a maximum of 5.1 km^2, with a mean of 1.4 ± 0.9 km^2, in the northern North Sea, and a maximum of 6.7 km^2 in the southern North Sea, with a mean of 2.0 ± 1.4 km^2 (Fig. 12). Our estimates derived from a multicomponent tidal analysis are in good agreement with the M2 tidal excursions estimates (Fig. 6a in Polton 2015), and estimates of horizontal displacements due to the M2 tide of 7.1 km in the southern and 1.8 km in the northern UK sectors (Thorpe 2012).

The tidal connectivity matrix derived from overlapping tidal footprints shows 900 connections exclud-

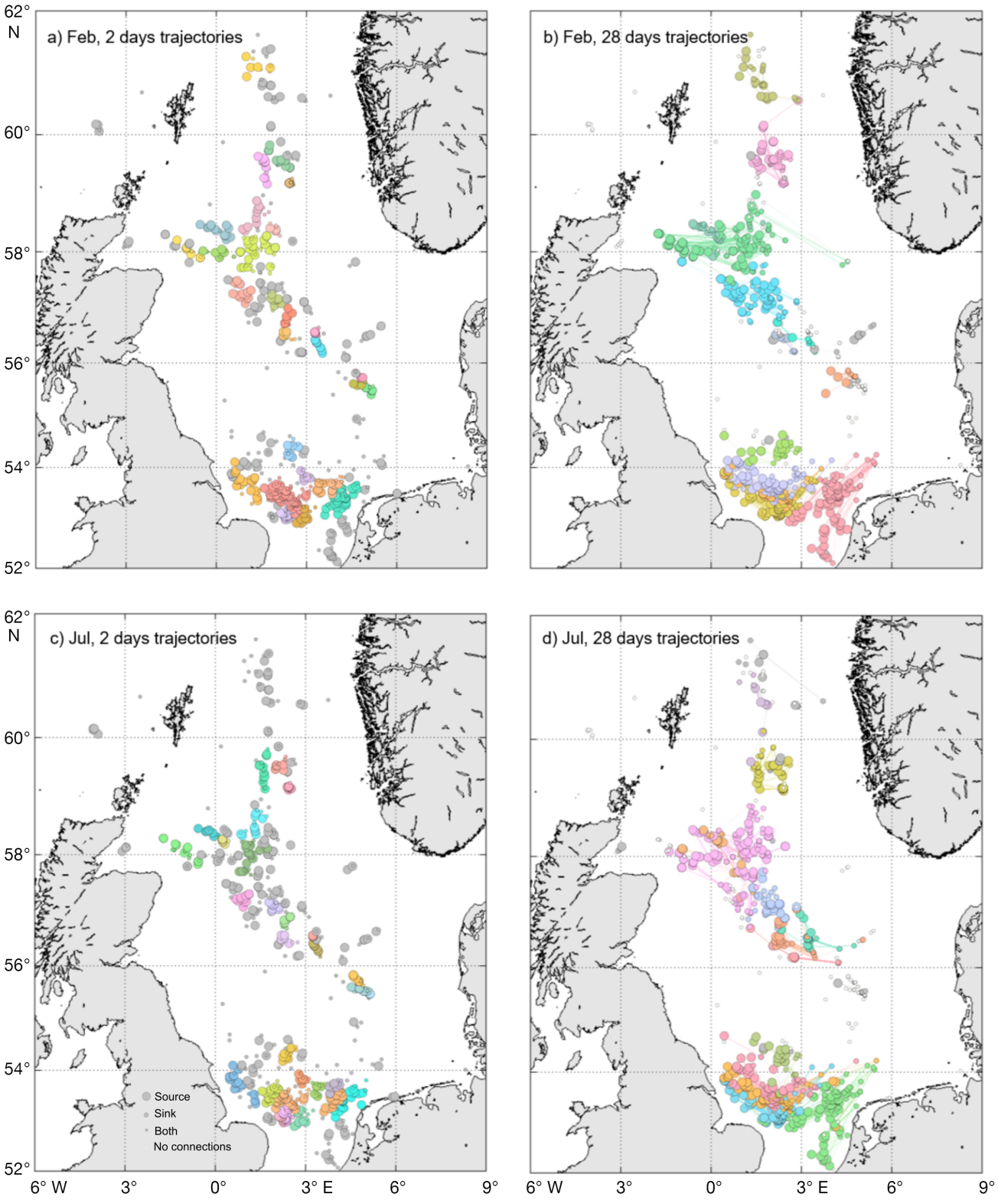

Fig. 11. Connectivity networks for the (a,b) February and (c,d) July particle tracking experiments considering (a,c) 2 d trajectories and (b,d) 28 d trajectories. Circle size identifies nodes acting predominantly as sources, sinks or equally as both, according to the key in panel c. Highly connected clusters identified by the modularity network metric including more than 1% of the platforms are shown in colour, grey circles identify platforms with fewer connections, and white circles in (b) and (d) those with none. For clarity, connecting lines are only shown in (b) and (d). See Section 2.3 for further details

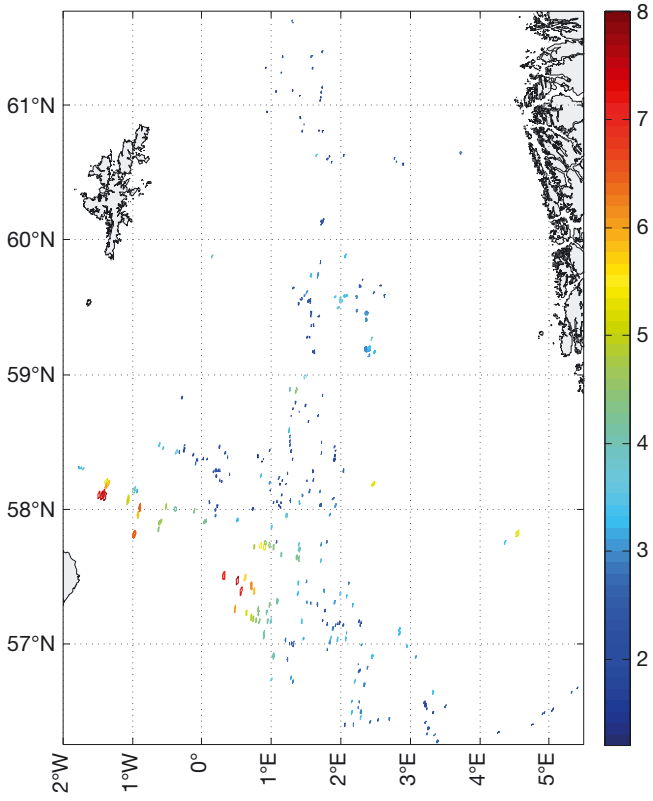

Fig. 12. Polygons representing the tidal footprint at each platform location coloured by the length of their major axis in kilometres for (a) the northern North Sea and (b) the central and southern North Sea

ing self-seeding, 0.2% of all possible structure-to-structure connections. A total of 39% of all the structures are tidally connected to at least one other structure: 36% of the northern North Sea structures and 42% of the southern North Sea structures. The north to south difference in the numbers of tidally connected structures is not as marked as the 23 vs. 60% (north vs. south) difference reported by Thorpe (2012) considering only the M2 tidal component.

The tidal connectivity matrix derived from overlapping tidal footprints is symmetrical (undirected), and self-seeding is always realized. This is in contrast to the full connectivity matrix derived from the particle tracking experiments, where 1-way connections between structures are possible (directed network), and self-seeding decreases exponentially with tracking time (Fig. 10). Similarly, all connections identified with the tidal footprint method are captured by the 2 d particle tracking experiments in both February and July, but this number decreases exponentially with tracking length, to <3% for 28 d trajectories. The degree network metric shows that the more highly connected structures are located in areas with a high density of structures (at 56.5 and 59.2° N), and connect to a maximum of 18 others in high proximity. Regions of medium tidal connectivity are located in the southwestern North Sea, and around 55.5° N (Fig. 13). The centrality metric (not shown) coincides with the high degree structures in the central and northern North Sea. Structures at 56.5° N are the only ones showing high betweenness (not shown).

4. DISCUSSION

4.1. Trade-offs of the methodology and approach

This study used a generalised approach to provide information on the dispersal potential of particles spreading from marine energy infrastructure in in the North Sea, and provides generalisable information about spatiotemporal scales of connectivity from oil and gas structures specifically. The analysis presented focusses on the near-surface layer where the currents are strongest to capture the maximum dispersal potential that could potentially minimize self-seeding. Strategically designed 3-dimensional advective Lagrangian passive particle experiments, spanning a large area and using high spatial resolution velocity fields (1.8 km) at high frequency (hourly), allowed us to describe the general patterns of dispersal among oil and gas structures in the entire North Sea. A minimum set up that allowed us to measure the scales of dispersal due to the main dynamics affecting shelf seas (tidal circulation and background mean currents) was defined. This setup includes near-surface particle releases at different tidal phases (same time of the day) during the 14 d spring–neap tidal cycle and seasonal releases during winter and summer. Treating the virtual particles as packets of larvae, and evaluating them for settlement repeatedly during the competency period allows for a robust calculation of connection strength while keeping the number of tracked particles at its minimum. In contrast to contemporary offline studies (e.g. Henry et al. 2018), these experiments were designed to highlight the dispersal of the simplest particles. To this end, random walk diffusion was not applied to the particles (as a parameterisation of unresolved motions). The principal reason for this decision was that, by using high-frequency model output with a sufficiently small grid scale, internal waves and eddies partially responsible for dispersal are directly resolved (Guihou et al. 2018), and are responsible for elevated levels of particle dispersal. However, smaller and unresolved scales remain, which are

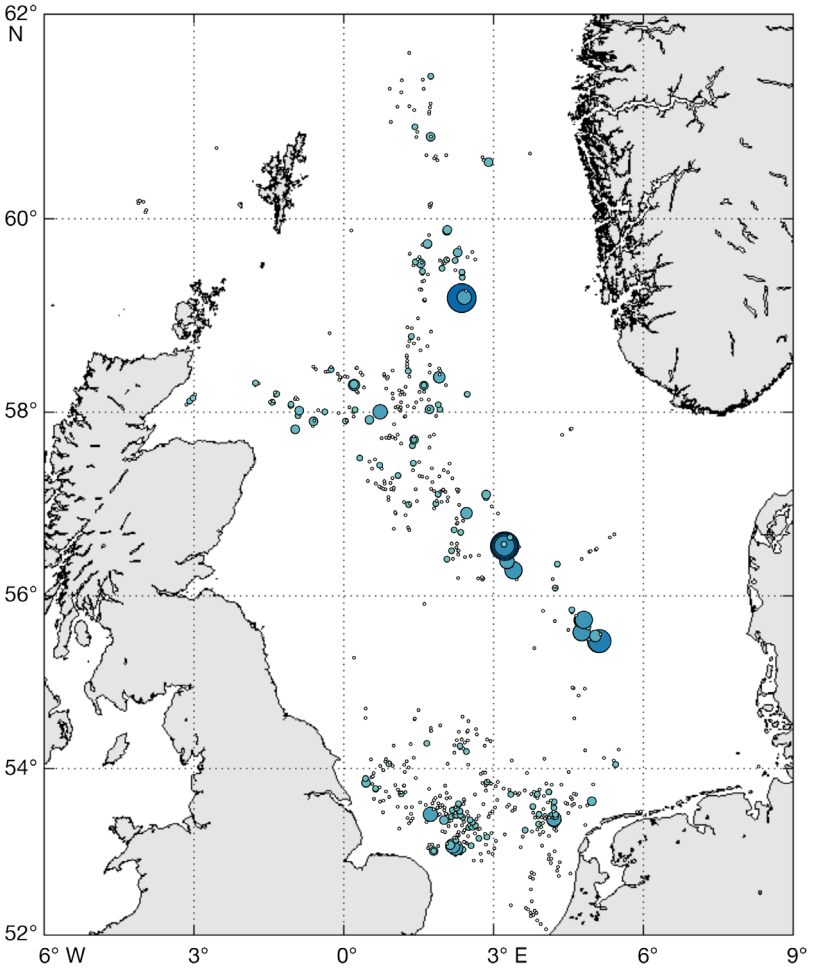

Fig. 13. Degree network metric of the tidal network. Both circle size and colour shade are proportional to the number of connections (degrees) of each structure. The smallest light circles represent no tidal connections, the smallest blue circles represent 2 connections, and the larger and darker circles represent 18 connections

omitted from these experiments and which could be parameterised by explicit diffusion and would likely increase the particle dispersion. However, since these results are broadly consistent with Thorpe (2012), further investigation is required to avoid double counting when adding explicit diffusion. Investigation into the relative contributions to particle dispersal by process across the range of length scales from microscale turbulence to the domain-scale residual flow remains an important and pressing problem. It is anticipated that progress could be made with an observational drifter pair release field campaign and a series of targeted process study simulations.

The particle tracking experiments were evaluated at different tracking durations to illustrate how connectivity varies depending on the time spent in the water. This is representative of how quickly materials decay, dilute or precipitate out of the water column, or (in the case of eggs and larvae) their PLD. It should be kept in mind that the use of neutrally buoyant passive particles is a generalisation and that non-neutrally buoyant particles (e.g. time-evolving biofouled microplastics, particulate organic matter) will have settling velocities that result in the trajectories deviating from those presented here. Furthermore, many marine species have specific larval behaviours with proven potential to alter their dispersal (Drake et al. 2013, Phelps et al. 2015b, Fox et al. 2016, Mayorga-Adame et al. 2017, Gary et al. 2020). However, confidence in the behaviours outside of laboratory conditions is limited (James et al. 2019). Therefore, while these results represent a step forward in our knowledge about North Sea connectivity, they can only be interpreted as indicative for specific particles and materials.

This study represents a step forward from the theoretical study by Thorpe (2012) and proposes a more generalised approach, in contrast to species-specific studies (e.g. Henry et al. 2018, van der Molen et al. 2018), and it is in agreement with their main findings of a highly interconnected ocean sprawl and strong potential for it to have an important ecological role.

4.2. Tidal connectivity

The tidal connectivity methodology presented is a novel way to estimate the scale of connectivity due to tidal advection that does not require particle tracking experiments. This approach is based solely on the harmonic analysis of the tidal signal, which is often available as output of ocean circulation models. It identifies connections that will occur during a tidal cycle, which varies for each tidal component included in the analysis, but for practical purposes, can be thought of as the period of the most important tidal components for the region of interest. In the North Sea, the M2 tide is dominant over most of the region, with a period of 12.42 h. This temporal scale is generally short in comparison to those of density- and wind-driven current transport. Tidal connectiv-

ity should be considered as a first approach to evaluate connectivity in places where tidal currents are dominant (i.e. southern North Sea) and for short dispersal periods, similar to the dominant tidal periods. The method allows differentiating between direct tidal connections, when 2 or more locations of interest fall within a tidal footprint polygon, and indirect tidal connections, when only the tidal polygons overlap. In a non-divergent flow, indirect tidal connections would not occur since particles would be oscillating across the tidal polygons in a synchronous way, which will prevent them from coming into contact with each other. In a more realistic ocean, it only takes a slight vertical displacement caused by the physical environment (i.e. vertical mixing, or vertical advection) or larval behaviour (i.e. buoyancy, vertical swimming) to break the tidal phase locking, which would cause exchange of particles between the indirectly connected polygons. The number of platforms connected at tidal scales is determined not only by the tidal footprints but also by the separation distance among platforms. In the presented case study, the length of the tidal polygons is often larger than the separation distance between oil and gas platforms (39% of all platforms are tidally connected), and therefore direct tidal connections are dominant (76.5%), while only 23.5% of all tidally connected platforms are indirectly connected. Given the short separation distance among subsea structures, larger numbers of tidally connected platforms (Fig. 13) are found in the central and northern North Sea, despite tidal footprints being half the size of those in the southern North Sea (Fig. 12).

The tidally connected scales derived from this novel and easy to apply method are comparable to those previously reported in the literature (see Section 3.3). The tidal footprint method is therefore a robust method to visualize rapid connectivity over a limited range. Tidal connections represent less than 1/3 of the connections generated by the 2 d trajectories, and these are restricted to short-range connections (radial dispersal distance <9 km; Fig. 12). Despite tidal currents being the strongest ubiquitous currents in the North Sea due to their oscillatory nature, they are incapable of producing long-distance connections; therefore, the resulting network is marginally interconnected at the larger spatial scale of the entire North Sea (Fig. 13). It is likely that processes like diffusion, sinking and behaviour, not included in the present study, would enhance both self-seeding and tidal connectivity, making this a conservative estimate.

Tidal connectivity is important for short time scale processes like rapidly maturing larvae, point-source released pollutants (e.g. Phelps et al. 2015a) that decay quickly or precipitate out of the water column to contaminate the seabed, or even search and rescue operations. Tidal footprints represent a good way to determine the settlement area around small structures like oil and gas platforms, as opposed to arbitrarily selecting a settlement radius, since it is valid to assume that once larvae are within a tidal footprint, tidal currents will make them sweep the footprint area, and reach the structures within it in a tidal cycle. Tidal footprints also provide a way of expanding the point source seeding area that the subsea structures represent. Materials emanating from them (i.e. pollutants or biological material) are rapidly spread by tides to cover an area, from which they are then carried away by density- and wind-driven currents. Particles could be released on the tidal footprint area to account for the initial tidal spread. Releasing particles in a wider area enhances the variability of pathways of the advected particles, and therefore the area swept by particles over time (dispersal) and their probability of encountering other artificial subsea structures or natural hard substrate (connectivity). This could be a remedial method for particle tracking experiments done with currents that do not include tides or misrepresent them due to their coarse temporal resolution (i.e. daily means). However, as tidal currents affect the dispersion in time-evolving ways (e.g. tidal dispersion of tracers, Bowden 1965; and locally modifying turbulence, e.g. Brereton et al. 2019), the full tidal effects would not be attained.

4.3. Ecological implications of the connectivity of oil and gas structures

The results presented here are a good starting point for the assessment of the connectivity and dispersal potential of various marine organisms associated with oil and gas infrastructure in the North Sea, or substances that could potentially emanate from them and can remain in the water up to 28 d. Common marine growth species in the Greater North Sea region with PLDs usually less than 28 d include the soft coral *Alcyonium digitatum* and the barnacles *Chirona hameri* and *Balanus crenatus*. In agreement with Coolen et al. (2020b), who studied both the genetical and modelled connectivity of the mussel *Mytilus edulis* in the southern North Sea, our findings indicate that the subsea structures in the entire North Sea are highly interconnected, particularly in the southern North Sea. Our study further identifies

several highly interconnected clusters along the basin, for both short (2 d) and long (28 d) PLDs, with fewer but larger clusters for the latter. Within the observed clusters, platforms serving as sources could be considered the most important for maintaining the populations established on oil and gas platforms, and the connectivity between them, while platforms acting as strong sinks represent populations that are more resilient. Platforms acting as both sources and sinks have the potential to serve as stepping stones for species to continue to expand to other structures, particularly those offshore, over several generations. They can be crucial for cross-basin connectivity of species that lack natural habitat offshore.

Both the decrease in numbers of unique connections when considering longer trajectories (Fig. 9) and the exponential decrease of self-seeding (Fig. 10) show how generally a higher proportion of longer-lived larvae are lost to unsuitable habitat, as they drift away from their source. Longer trajectories, however, increase the probability of long-distance connections, creating an overall more interconnected basin-wide network. Our case study clearly illustrates the ecological trade-off between closed populations with high local recruitment, susceptible to local environmental pressure, and open populations with lower recruitment but longer-distance connectivity leading to colonisation of new habitats and strong genetic variability (Cowen et al. 2000). Both small- and large-scale connectivity are present and linked to PLD. In terms of species of conservation interest that colonise energy infrastructure (e.g. the protected reef framework-forming coral *Lophelia pertusa*), a decision-maker may want to encourage connectivity over the large scale. In contrast, in terms of mitigating risks associated with the large-scale spreading of non-native or invasive species, if these are found already on a cluster of structures close together, a decision-maker might want to discourage new structures being added nearby that could make the network wider, considering the risks of open populations having the potential to spread species further afield.

Platforms directly connected by tides could be considered redundant in terms of their contribution to the connectivity of the network, in which case other ecological and operational aspects like species distribution and abundance, distance to shore and maintenance feasibility should be taken into account to determine which platforms should be kept or removed. For operational proposes, to determine if specific structures should be removed or kept in place and maintained over time to preserve its ecological function, a more detailed study, with a multispecies biological connectivity approach, in the region of interest would be required. A more in-depth investigation of the generated networks is recommended, as well as the application of methods specifically designed to address this issue like those developed by Fox et al. (2019). These investigations are computationally demanding; here we have dedicated computational resources to establishing a synopsis of a wide area, rather than (for example) investigating a long simulation for a small region, or targeting the spread of a specific species.

4.4. Expected effects of interannual variability and climate change

The NAO has a strong influence on the North Sea circulation. The flow strength during years with a negative winter NAO Index are significantly weaker than those with positive NAO Index (Schrum & Sigismund 2001 in Sündermann & Pohlmann 2011) due to the suppression of westerly winds (Chafik 2012, Woollings et al. 2015). A previous study by Fox et al. (2016) showed that connectivity among North Atlantic marine protected areas is strongly correlated to the NAO, with positive NAO phase conditions producing a well-connected but asymmetrical network connected from west to east, while the negative NAO phase produced reduced connectivity. The present study uses modelled currents of 2010, a strongly negative NAO year; therefore, the described circulation, trajectory pathways and connectivity patterns reported here could be assumed to be a conservative 'base-case' estimate, since westerly winds and inflow from the Atlantic were suppressed by the negative NAO conditions. Another study focussed on larval connectivity of the deepwater coral *L. pertusa*, restricted to oil and gas structures in the northern North Sea (Henry et al. 2018), addressed inter-annual variability over a 3 yr period that encompassed the transition from a strong negative (2010) to a positive NAO state (2012). The evolution of connectivity throughout the 3 years broadly conformed to an increase in zonal connections from west to east and a reduction of meridional connections when transitioning from negative (2010) to positive (2011 and 2012) NAO phase. The networks presented here are expected to show similar interannual variability changes in positive NAO phases, particularly in the northern North Sea. Mathis et al. (2015) documented higher NAO correlations in the northern North Sea than in the southern parts; therefore changes are expected to be

more subtle in the already strongly connected southern North Sea. Exploring interannual variability and the effects of extreme events and climate-induced changes in the North Sea circulation on the connectivity patterns of oil and gas structures is needed to determine the bounds of the scales of dispersal and connectivity presented here. Metrics like maximum linear dispersal distance are expected to be particularly sensitive. Expanding this research to investigate sensitivity to interannual variability and climate change are further steps for this research, as well as the interactions with other man-made structures including wind farms, wrecks and natural hard substrate habitat, similarly to a study by van der Molen et al. (2018), but with higher spatiotemporal resolution.

Increased permanent stratification in the ocean is a robust outcome of future climate projections (Capotondi et al. 2012). Seasonal changes in stratification on shelf seas are much less robust (Tinker et al. 2016, Holt et al. 2018). For the North Sea, this may imply more uniform conditions with an expansion of the northern environment, which shows stronger seasonal and inter-annual variability, and shrinkage of the well-mixed, tidal-dominated southern North Sea conditions. There is still a degree of uncertainty on how climate change will affect the circulation of the North Sea; however, it seems to be one of the more susceptible shelf seas (Kauker 1998, Langenberg et al. 1999, Holt et al. 2016). Expected changes in stratification, circulation patterns and flow strength will undoubtedly alter connectivity. This would have significant ecosystem impacts, since commercially and ecologically important species have life cycles coupled to the North Sea circulation, such as herring larvae, which rely on cyclonic circulation for transport from spawning to nursery grounds (Corten 2013), and the deep-water coral *L. pertusa*, which has an interconnected population associated with oil and gas structures (Henry et al. 2018). Increased water temperatures in the future ocean are likely to affect organisms physiologically, which will in turn imply modifications to the biological parameters crucial to model larval dispersal such spawning times and PLD and larval behaviour (e.g. Pankhurst & Munday 2011). The potentially synergistic effects of climate change on both the physical and biological processes involved in larval connectivity make it difficult to estimate uncertainty around future connectivity patterns. Future ocean conditions would need to be taken into account if a long-term conservation strategy, similar to the rigs-to-reef programme (Macreadie et al. 2011), is adopted as part of the decommissioning strategy for the oil and gas structures in the North Sea.

5. CONCLUSION

This study focusses on a generalist approach to investigate the connectivity among oil and gas structures in the North Sea; as such, it can serve as a starting point for more specialized studies, like those focussing on specific species, pollution dispersal, impacts of adding marine renewable infrastructure, etc. It presents a strategically designed, yet generic and minimalistic approach to characterize dispersal and connectivity. Particle tracking in a high-resolution model is combined with a new method to evaluate tidally driven connectivity. This tidal analysis approach is put forward as a quick and easily relocatable approach to evaluate ground-zero tidal connectivity in shelf seas where the tide plays a prominent role. Together these form a relocatable approach of scalable complexity that considers the most important physical drivers of dispersal in coastal shelf seas while keeping computing requirements at a minimum.

Our approach highlights considerable spatial variability in dispersal between the northern (deep and stratified) region versus the southern (shallow and well-mixed) region, and temporal variability between the mixed and energetic winter season and the stratified and quieter summertime, with the marked regional sensitivity to seasonality explained by stratification. At least 1 in 5 of the connections realized at short PLDs are due to tidal dispersal and are identified by the new tidal connectivity analysis, representing an important baseline to assess the ecological implications of structure removal or demonstrate the need for more detailed modelling work.

Questions of decommissioning, leaving structures in place or even rigs-to-reefs projects in the North Sea are very contentious. This research adds to the growing body of information assessing the contribution of basin-wide spatiotemporal scales and patterns of network connectivity to the ecological role of subsea man-made structures in the North Sea. We do not attempt here to assess the ecological value of the populations using these structures, but to provide tools, and an example of their use, to help assess the resilience of these populations to changes in the topology of these manmade networks.

Data availability. Oil and gas platform locations were obtained from the OSPAR Data and Information Management System (https://odims.ospar.org/en/submissions/ospar_offshore_installations_2015_01/). The LTRANSforNEMO code used to perform the particle tracking experiments is available at https://doi.org/10.5281/zenodo.6092322. Input data and the data that support the findings of this study are available on request from the corresponding author.

Acknowledgements. This study was conducted in the Appraisal of Network Connectivity for North Sea subsea oil and gas platforms (ANChor) project. This was an Oil and Gas UK led Joint Industry Project, in the Influence of Structures In The Ecosystem (INSITE) programme. We acknowledge support from the following projects while writing and revising the manuscript: C.G.M.-A. was additionally supported by the National Environmental Research Council (NERC) under the 'Resolving Climate Impacts on shelf and Coastal sea Ecosystems' (ReCICLE; NE/M003477/1) and 'Climate Linked Atlantic Sector Science' (CLASS; NERC Marine National Capability) projects. J.A.P. was also additionally supported by NERC under CLASS. L.-A.H. received funding from the European Union's Horizon 2020 research and innovation programme under grant agreement no. 818123 (iAtlantic). This output reflects only our views, and the European Union cannot be held responsible for any use that may be made of the information contained therein. We thank Dr. Jason Holt for his constructive feedback on an earlier version of this manuscript.

LITERATURE CITED

Abelson A, Denny M (1997) Settlement of marine organisms in flow. Annu Rev Ecol Syst 28:317–339

Bastian M, Heymann S, Jacomy M (2009) Gephi: an open source software for exploring and manipulating networks. 2. International AAAI Conference on Weblogs and Social Media. https://gephi.org/publications/gephi-bastian-feb09.pdf

Blondel VD, Guillaume JL, Lambiotte R, Lefebvre E (2008) Fast unfolding of communities in large networks. J Stat Mech 2008:P10008

Bowden KF (1965) Horizontal mixing in the sea due to a shearing current. J Fluid Mech 21:83–95

Brereton A, Tejada-Martínez AE, Palmer MR, Polton JA (2019) The perturbation method — a novel large-eddy simulation technique to model realistic turbulence: application to tidal flow. Ocean Model 135:31–39

Brown J, Hill AE, Fernand L, Horsburgh KJ (1999) Observations of a seasonal jet-like circulation at the central North Sea cold pool margin. Estuar Coast Shelf Sci 48:343–355

Capotondi A, Alexander MA, Bond NA, Curchitser EN, Scott JD (2012) Enhanced upper ocean stratification with climate change in the CMIP3 models. J Geophys Res Oceans 117:C04031

Chafik L (2012) The response of the circulation in the Faroe-Shetland Channel to the North Atlantic Oscillation. Tellus A Dyn Meteorol Oceanogr 64:18423

Claisse JT, Pondella DJ, Love M, Zahn LA, Williams CM, Williams JP, Bull AS (2014) Oil platforms off California are among the most productive marine fish habitats globally. Proc Natl Acad Sci USA 111:15462–15467

Coolen JWP, van der Weide B, Cuperus J, Blomberg M and others (2020a) Benthic biodiversity on old platforms, young wind farms, and rocky reefs. ICES J Mar Sci 77: 1250–1265

Coolen JWP, Boon AR, Crooijmans R, van Pelt H and others (2020b) Marine stepping-stones: connectivity of *Mytilus edulis* populations between offshore energy installations. Mol Ecol 29:686–703

Corten A (2013) Recruitment depressions in North Sea herring. ICES J Mar Sci 70:1–15

Cowen RK, Lwiza KMM, Sponaugle S, Paris CB, Olson DB (2000) Connectivity of marine populations: open or closed? Science 287:857–859

Creed JC, Fenner D, Sammarco P, Cairns S and others (2017) The invasion of the azooxanthellate coral *Tubastraea* (Scleractinia: Dendrophylliidae) throughout the world: history, pathways and vectors. Biol Invasions 19: 283–305

Drake PT, Edwards CA, Morgan SG, Dever EP (2013) Influence of larval behavior on transport and population connectivity in a realistic simulation of the California Current System. J Mar Res 71:317–350

Fowler AM, Macreadie PI, Jones DOB, Booth DJ (2014) A multi-criteria decision approach to decommissioning of offshore oil and gas infrastructure. Ocean Coast Manag 87:20–29

Fowler AM, Jørgensen AM, Svendsen JC, Macreadie PI and others (2018) Environmental benefits of leaving offshore infrastructure in the ocean. Front Ecol Environ 16: 571–578

Fox AD, Henry LA, Corne DW, Roberts JM (2016) Sensitivity of marine protected area network connectivity to atmospheric variability. R Soc Open Sci 3:160494

Fox AD, Corne DW, Mayorga Adame CG, Polton JA, Henry LA, Roberts JM (2019) An efficient multi-objective optimization method for use in the design of marine protected area networks. Front Mar Sci 6:17

Gary SF, Fox AD, Biastoch A, Roberts JM, Cunningham SA (2020) Larval behaviour, dispersal and population connectivity in the deep sea. Sci Rep 10:10675

Gates AR, Benfield MC, Booth DJ, Fowler AM, Skropeta D, Jones DOB (2017) Deep-sea observations at hydrocarbon drilling locations: contributions from the SERPENT Project after 120 field visits. Deep Sea Res II 137:463–479

Gawarkiewicz G, Monismith S, Largier J (2007) Observing larval transport processes affecting population connectivity: progress and challenges. Oceanography 20:40–53

Guihou K, Polton J, Harle J, Wakelin S, O'Dea E, Holt J (2018) Kilometric scale modeling of the North West European shelf seas: exploring the spatial and temporal variability of internal tides. J Geophys Res Oceans 123: 688–707

Henry LA, Mayorga-Adame CG, Fox AD, Polton JA and others (2018) Ocean sprawl facilitates dispersal and connectivity of protected species. Sci Rep 8:11346

Hill AE, Brown J, Fernand L, Holt J and others (2008) Thermohaline circulation of shallow tidal seas. Geophys Res Lett 35:L11605

Holt J, Proctor R (2008) The seasonal circulation and volume transport on the northwest European continental shelf: a fine-resolution model study. J Geophys Res 113:C06021

Holt J, Schrum C, Cannaby H, Daewel U and others (2016) Potential impacts of climate change on the primary production of regional seas: a comparative analysis of five European seas. Prog Oceanogr 140:91–115

Holt J, Polton J, Huthnance J, Wakelin S and others (2018) Climate-driven change in the North Atlantic and Arctic Oceans can greatly reduce the circulation of the North Sea. Geophys Res Lett 45:11827–11836

Huthnance JM (1997) North Sea interaction with the North Atlantic Ocean. Dtsche Hydrogr Z 49:153–162

James MK, Polton JA, Brereton AR, Howell KL, Nimmo-Smith WAM, Knights AM (2019) Reverse engineering field-derived vertical distribution profiles to infer larval swimming behaviors. Proc Natl Acad Sci USA 116: 11818–11823

Kauker F (1998) Regionalization of climate model results for the North Sea. PhD thesis, University of Hamburg

Kendon M, McCarthy M (2015) The UK's wet and stormy winter of 2013/2014. Weather 70:40–47

Lambiotte R, Delvenne JC, Barahona M (2009) Laplacian dynamics and multiscale modular structure in networks. IEEE Trans Netw Sci Eng 1:76–90

Langenberg H, Pfizenmayer A, von Storch H, Sündermann J (1999) Storm-related sea level variations along the North Sea coast: natural variability and anthropogenic change. Cont Shelf Res 19:821–842

Leis JM, Carson-Ewart BM (1999) *In situ* swimming and settlement behaviour of larvae of an Indo-Pacific coral-reef fish, the coral trout *Plectropomus leopardus* (Pisces: Serranidae). Mar Biol 134:51–64

Love MS, Schroeder DM, Lenarz W, MacCall A, Bull AS, Thorsteinson L (2006) Potential use of offshore marine structures in rebuilding an overfished rockfish species, bocaccio (*Sebastes paucispinis*). Fish Bull 104:383–390

Macreadie PI, Fowler AM, Booth DJ (2011) Rigs-to-reefs: Will the deep sea benefit from artificial habitat? Front Ecol Environ 9:455–461

Mathis M, Elizalde A, Mikolajewicz U, Pohlmann T (2015) Variability patterns of the general circulation and sea water temperature in the North Sea. Prog Oceanogr 135: 91–112

Mayorga-Adame CG, Batchelder HP, Spitz YH (2017) Modeling larval connectivity of coral reef organisms in the Kenya-Tanzania region. Front Mar Sci 4:92

McLean DL, Ferreira LC, Benthuysen JA, Miller KJ and others (2022) Influence of offshore oil and gas structures on seascape ecological connectivity. Glob Change Biol (in press) doi:10.1111/gcb.16134

North EW, Schlag Z, Adams EE, Sherwood CR, He R, Hyun H, Socolofsky SA (2011) Simulating oil droplet dispersal from the *Deepwater Horizon* spill with a Lagrangian approach. In: Liu Y, Macfadyen A, Ji ZG, Weisberg RH (eds) Monitoring and modeling the *Deepwater Horizon* oil spill: a record breaking enterprise. American Geophysical Union, Geophysical Monograph Series 195:217–226

Otto L, Zimmerman JTF, Furnes GK, Mork M, Saetre R, Becker G (1990) Review of the physical oceanography of the North Sea. Neth J Sea Res 26:161–238

Pajuelo JG, González JA, Triay-Portella R, Martín JA, Ruiz-Díaz R, Lorenzo JM, Luque Á (2016) Introduction of non-native marine fish species to the Canary Islands waters through oil platforms as vectors. J Mar Syst 163:23–30

Pankhurst NW, Munday PL (2011) Effects of climate change on fish reproduction and early life history stages. Mar Freshw Res 62:1015–1026

Phelps JJC, Blackford JC, Holt JT, Polton JA (2015a) Modelling large-scale CO_2 leakages in the North Sea. Int J Greenh Gas Control 38:210–220

Phelps JJC, Polton JA, Souza AJ, Robinson LA (2015b) Behaviour influences larval dispersal in shelf sea gyres: *Nephrops norvegicus* in the Irish Sea. Mar Ecol Prog Ser 518:177–191

Polton JA (2015) Tidally induced mean flow over bathymetric features: a contemporary challenge for high-resolution wide-area models. Geophys Astrophys Fluid Dyn 109:207–215

Quante M, Colijn F, Bakker JP, Härdtle W and others (2016) Introduction to the assessment — characteristics of the region. In: Quante M, Colijn F (eds) North Sea region climate change assessment. Regional Climate Studies, Springer International Publishing, Cham, p 1–52

Robinson DP, Jaidah MY, Jabado RW, Lee-Brooks K and others (2013) Whale sharks, *Rhincodon typus*, aggregate around offshore platforms in Qatari waters of the Arabian Gulf to feed on fish spawn. PLOS ONE 8:e58255

Simpson JH (1981) The shelf-sea fronts: implications of their existence and behaviour. Philos Trans R Soc Lond A 302: 531–546

Sündermann J, Pohlmann T (2011) A brief analysis of North Sea physics. Oceanologia 53:663–689

Thorpe SA (2012) On the biological connectivity of oil and gas platforms in the North Sea. Mar Pollut Bull 64:2770–2781

Tinker J, Lowe J, Pardaens A, Holt J, Barciela R (2016) Uncertainty in climate projections for the 21st century northwest European shelf seas. Prog Oceanogr 148:56–73

Todd VLG, Pearse WD, Tregenza NC, Lepper PA, Todd IB (2009) Diel echolocation activity of harbour porpoises (*Phocoena phocoena*) around North Sea offshore gas installations. ICES J Mar Sci 66:734–745

Torquato F, Jensen HM, Range P, Bach SS and others (2017) Vertical zonation and functional diversity of fish assemblages revealed by ROV videos at oil platforms in The Gulf. J Fish Biol 91:947–967

Van der Molen J, García-García LM, Whomersley P, Callaway A, Posen PE, Hyder K (2018) Connectivity of larval stages of sedentary marine communities between hard substrates and offshore structures in the North Sea. Sci Rep 8:14772

Vörösmarty CJ, Fekete BM, Meybeck M, Lammers RB (2000) Global system of rivers: Its role in organizing continental land mass and defining land-to-ocean linkages. Glob Biogeochem Cycles 14:599–621

Winther NG, Johannessen JA (2006) North Sea circulation: Atlantic inflow and its destination. J Geophys Res Oceans 111:C12018

Woollings T, Franzke C, Hodson DLR, Dong B, Barnes EA, Raible CC, Pinto JG (2015) Contrasting interannual and multidecadal NAO variability. Clim Dyn 45:539–556

Young WR, Rhines PB, Garrett CJR (1982) Shear-flow dispersion, internal waves and horizontal mixing in the ocean. J Phys Oceanogr 12:515–527

Editorial responsibility: Alejandro Gallego, Aberdeen, UK
Reviewed by: 2 anonymous referees

Submitted: June 2, 2021
Accepted: November 30, 2021
Proofs received from author(s): February 16, 2022